Article

Low-Temperature, Efficient Synthesis of Highly Crystalline Urchin-like Tantalum Diboride Nanoflowers

Delei Liu [1], Jianghao Liu [1,*], Peikan Ye [1], Haijun Zhang [1,*] and Shaowei Zhang [2]

[1] The State Key Laboratory of Refractories and Metallurgy, Wuhan University of Science and Technology, Wuhan 430081, China; 15927529267@163.com (D.L.); yepk2022@126.com (P.Y.)
[2] College of Engineering, Mathematics and Physical Sciences, University of Exeter, Exeter EX4 4QF, UK; s.zhang@exeter.ac.uk
* Correspondence: liujianghao2014@wust.edu.cn (J.L.); zhanghaijun@wust.edu.cn (H.Z.)

Abstract: Urchin-like tantalum diboride (TaB_2) nanoflowers were successfully synthesized via a high-efficiency and energy-saving methodology, molten-salt and microwave co-modified boro/carbothermal reduction, using less expensive B_4C as a reducing agent. By taking advantage of the synergistic effects of the molten-salt medium and microwave heating conditions, the onset formation temperature of TaB_2 was drastically reduced to below 1000 °C, and phase-pure powders of TaB_2 nanoflowers were obtained at temperatures as low as 1200 °C within only 20 min. Notably, the present temperature conditions were remarkably milder than those (>1500 °C for several hours) required by conventional reduction methods, which use the strong, but expensive, reducing agent, elemental boron. The resulting urchin-like TaB_2 nanoflowers consisted of numerous uniform single-crystalline nanowires with lengths up to 4.16 μm, and high aspect ratios >10. This result indicated that the as-synthesized urchin-like TaB_2 nanoflowers possessed high specific surface area and anisotropic morphology, which were favorable not only for sintering, but also for toughening their bulk counterparts.

Keywords: ultra-high-temperature ceramics; tantalum diboride; microwave; molten-salt synthesis; single crystal; urchin-like; nanoflower; toughening

1. Introduction

As one of the most important ultra-high-temperature ceramics (UHTCs) for potential applications at >2000 °C, tantalum diboride (TaB_2) has attracted extensive interest in recent decades due to its rapidly rising demand for high-end structural applications in harsh environments, such as the propulsion systems in new-generation space vehicles, combustion chambers of rockets, and the leading edge of reentry hypersonic missiles [1–3]. Under such extreme operating conditions, the frequent occurrence of sharp heating–cooling cycles results in high thermal stress in TaB_2-based protective materials, greatly challenging their thermal shock resistance as well as the relevant main factor, fracture toughness [4,5]. Thus, it is of significant importance to prepare monolithic TaB_2 with sufficient fracture toughness.

To overcome the poor toughness of many ceramics, the introduction of a secondary reinforcement phase with an anisotropic (e.g., rod- or plate-like) morphology into the ceramic matrix has been demonstrated to be effective [6,7]. Nevertheless, due to the ultra-high service temperature, the number of the second-phase candidates applicable to TaB_2-based materials was extremely limited. Considering this, "self-toughening" was regarded as the only feasible way to enhance the fracture toughness of TaB_2-based materials [8]. Thus, their powder counterparts, consisting of highly crystalline anisotropy-shaped TaB_2 particles, were perceived to be desirable for preparation of high-performance TaB_2-based materials [9–12].

Unfortunately, with the boro/carbothermal reduction methodology conventionally utilized for the industrial preparation of TaB_2 and other raw powders of UHTCs as well as TaB_2, it was still a challenging task to endow the powder product with anisotropic

morphology and the resulting potential for toughness enhancement [13,14]. Additionally, the preparation of TaB$_2$ powders via conventional thermal reduction commonly necessitates severe temperature conditions, including high firing temperature (>1500 °C) and long dwelling time (dozens of hours), which not only dramatically increases corresponding energy and time consumptions, but also seriously deteriorates the sinterability of the powder product. For instance, Guo et al. synthesized TaB$_2$ with amorphous morphology using the conventional borothermal reduction (BTR) at temperatures as high as 1550 °C for one hour, by using highly expensive elemental boron as both B source and reducing agent [13]. Zhang et al. successfully prepared TaB$_2$ powders by heating the raw powders of Ta$_2$O$_5$, B$_4$C and graphite at 1600 °C, albeit both needle-like and rounded particles coexisted in the final product [15]. In summation, the current thermal-reduction-based methodology for mass preparation of TaB$_2$ powders suffers from the drawbacks of high preparation cost and poor quality of products, which are mainly attributable to the intrinsically low diffusion coefficient of TaB$_2$ and the resulted low rates of both synthetic reaction and crystal growth [16].

In this view, the prospect of introducing a liquid phase was deemed promising for improving the diffusion rate of TaB$_2$, and therefore enhancing its synthesis and epitaxial crystal growth. For instance, Ren et al. exploited low-melting-point Ta-B-C-O precursors to supply the boro/carbothermal reduction reaction for synthesizing TaB$_2$ with liquid medium. However, no formation of anisotropic TaB$_2$ was not reported despite the requirement of a high processing temperature of 1500 °C was still demanded, which was considered to be mainly due to the decomposition loss of the low-melting-point organic-based medium, before the temperature desirable for crystal growth of TaB$_2$ was attained [17]. As a result, inorganic salt with a relatively higher melting point was regarded as a promising medium for solid-state synthetic reaction of high-temperature materials, including TaB$_2$. For instance, Ran et al. utilized the molten-salt-assisted BTR method to prepare rod-like TaB$_2$ powders after a one-hour dwelling period at a reduced temperature of 1000 °C, albeit the requirement of a large amount of boron powders resulted in high material costs [18].

In addition, microwaves have also been verified to be capable of effectively accelerating not only synthetic reactions, but also crystal growth of high-temperature materials. Moreover, it was attainable for the microwave field to cooperate with the molten-salt field, therefore jointly enhancing the thermodynamic favorability of synthetic reactions and facilitating self-assembly of anisotropic-shaped crystals [19,20]. Accordingly, in our previous research, microwaves were utilized to further modify the molten-salt-assisted BCTR method to prepare ZrB$_2$ and ZrB$_2$-SiC powders with anisotropic morphologies under much milder conditions [21,22].

Consequently, in this work, molten-salt and microwave comodified boro/carbothermal reduction was developed for synthesizing TaB$_2$, using Ta$_2$O$_5$ and B$_4$C as raw materials. The effects of various important parameters on the synthesis of TaB$_2$ were elaborately regulated to save energy and efficiently prepare single-phase TaB$_2$ powders with high specific surface area and anisotropic morphology.

2. Materials and Methods

2.1. Raw Materials

The raw materials of tantalum oxide (Ta$_2$O$_5$; purity > 98.5%; average particle size of 0.39 μm; Shanghai Aladdin Bio-Chem Technology Co., Ltd., Tianjin, China) and boron carbide (B$_4$C; purity > 98.0%; average particle size of 3.74 μm; Mudanjiang Jingangzuan Boron-Carbide Co., Ltd., Mudanjiang, China) were used as received for synthesis of TaB$_2$. Salts of sodium chloride and potassium chloride (NaCl and KCl; purities > 99.9%; Bodi Chem. Co., Ltd., Tianjin, China) were used as a reacting medium. All above reagents were directly used without further purification or modification.

$$7Ta_2O_5(s) + 11B_4C(s) = 14TaB_2(s) + 8B_2O_3(l) + 11CO(g) \tag{1}$$
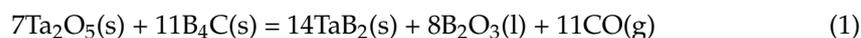
For compensating for the volatilization loss of boron species during the synthetic reaction of TaB_2, certain excess amounts of B_4C were added into the raw material powders (according to reaction (1)). For the reacting medium, the molar ratio between NaCl and KCl was fixed at 1:1. The batch compositions and processing parameters for the molten-salt and microwave-assisted boro/carbothermal reduction (MSM-BCTR) and the conventional BCTR are listed in Table 1. The corresponding products are labeled as MSMBC-(1–7).

Table 1. Batch compositions and processing parameters for synthesis of TaB_2 by either MSM-assisted or conventional BCTR method.

Sample No.	Molar Ratio		Heating Mode	Temperature (°C)	Dwelling Time (min)	Salt Medium
	Ta_2O_5	B_4C				
MSMBC-1	1.0	2.9	MWH [a]	1000	20	NaCl/KCl
MSMBC-2	1.0	2.9	MWH	1100	20	NaCl/KCl
MSMBC-3	1.0	2.9	MWH	1200	20	NaCl/KCl
MSMBC-4	1.0	2.8	MWH	1200	20	NaCl/KCl
MSMBC-5	1.0	3.0	MWH	1200	20	NaCl/KCl
MSMBC-6	1.0	2.9	MWH	1200	20	—
MSMBC-7	1.0	2.9	CH [b]	1200	20	NaCl/KCl

[a,b] MWH and CH denote microwave heating and conventional heating processes, respectively.

2.2. Experiment Procedure

Similar to a typical MSM-BCTR process for synthesizing TaB_2, the reactants, consisting of Ta_2O_5/B_4C and the salt mixture of NaCl/KCl in a weight ratio of 1:2, were initially mixed in a corundum crucible. Then, the crucible, contained by a SiC saggar, was positioned in the heating area of a microwave furnace (HAMiLab-V3000; 3 kW; 2.45 GHz; Changsha Longtech Co., Ltd., Changsha, China). The space between the saggar and crucible was filled with green silicon carbide powders to facilitate the microwave heating of the raw material powders, and the operating temperature was monitored in real-time by an infrared thermometer. Afterwards, in a flowing argon atmosphere, the raw material powders were heated at a constant rate of 10 °C/min to the preset temperature range of 1000–1200 °C, then held for 0–20 min before cooling naturally to the ambient temperature. The resultant powders were ground and repeatedly rinsed with deionized water to completely remove the residual salt, followed by overnight drying in a vacuum oven at 80 °C, before undergoing the following characterization and testing.

2.3. Characterization and Testing

Phase compositions of the powder products were examined by X-ray diffraction (XRD, Empyrean, PANalytical, Almelo, The Netherlands) with $CuK\alpha$ radiation (λ = 0.1542 nm). The morphology and microstructure of as-obtained TaB_2 powders were characterized using a field-emission scanning electron microscope (FE-SEM, Nova400NanoSEM, Philips, Amsterdam, The Netherlands) equipped with an energy dispersive spectrometer (EDS) and transmission electron microscope (TEM, JEM-2100UHRSTEM, JEOL, Tokyo, Japan), and their mean aspect ratio was estimated based on the measurements of at least 200 well-grown rod-like particles.

3. Results

As confirmed by our previous researchers [21,22], the present MSM-BCTR method was capable of greatly accelerating the BCTR reaction for synthesizing boron-based UHTCs at reduced temperatures. Therefore, the syntheses of TaB_2 were performed at a relatively low temperature range of 1000–1200 °C, for an identical dwelling time of 20 min, with batch powder composition $n(B_4C)/n(Ta_2O_5)$ = 2.9, and weight ratio between salts and reactants of m_s/m_r = 2.0. Specifically, as the firing temperature reached 1000 °C (Figure 1), although there existed a lot of un-reacted Ta_2O_5 and B_4C, as well as the intermediate product of TaO_2 (produced by partial reduction of Ta_2O_5), in the final product (MSMBC-1), a minor

amount of TaB_2 could also be identified. This result indicated that the expected formation reaction of TaB_2 (reaction (1)) was initiated at a temperature lower than 1000 °C, which was dramatically lower than that (up to 1550 °C) required by the conventional BCTR method using an identical type of reducing agent [9]. Subsequently, on increasing the temperature to 1100 °C (MSMBC-2), the intensities of the diffraction peaks belonging to TaB_2 increased, while those of the residual reactants and intermediate product accordingly decreased, revealing the rising temperature had a positive effect on enhancing the synthesis of TaB_2. More interestingly, upon further increasing temperature to 1200 °C, all observable diffraction peaks of the product (MSMBC-3) were indexed to TaB_2, demonstrating that phase-pure TaB_2 powders were successfully obtained. This result verified that, although the temperature was as low as 1200 °C, the synthetic reaction of TaB_2 was still highly efficient, remarkably superior to that (at least one hour) in the conventional BCTR using the stronger reducing agent, boron [18].
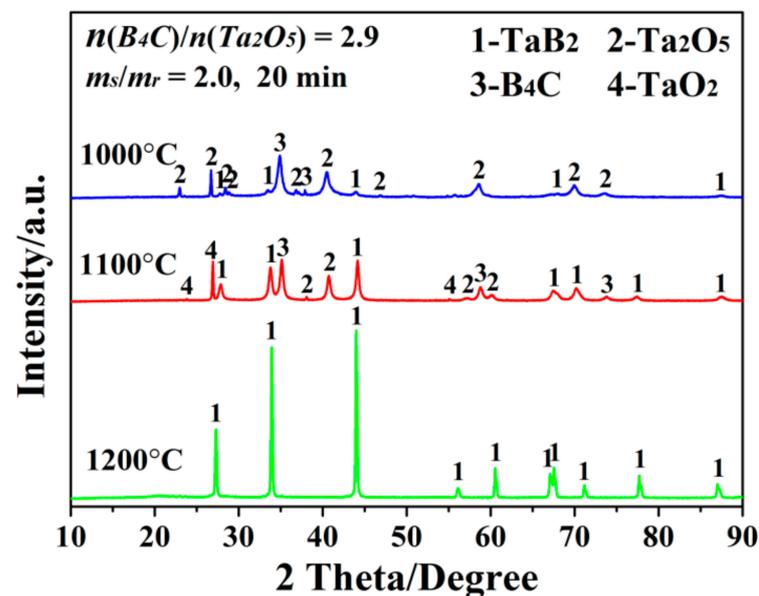

Figure 1. XRD patterns of the samples resultant from MSM-BCTR treatments at 1000–1200 °C/20 min, with the identical processing parameters of $n(B_4C)/n(Ta_2O_5)$ = 2.9 and m_s/m_r = 2.0.

Moreover, the additional amount of reducing agent was deemed another key factor that greatly influenced the synthetic result of TaB_2, because insufficient dosages of reducing agent would have impeded the expected completion of the synthetic reaction, while excessive dosages would have induced carbon residue in the final product, seriously and irreversibly deteriorating its purity and sinterability. Given this, the following experiments were performed using different addition amounts of B_4C in the original powder batches. On one hand, as shown in Figure 2, in sharp contrast with MSMBC-3 (composed of single-phase TaB_2), the sample (MSMBC-4) prepared under identical processing conditions, but with a slightly less amount of B_4C (with the ratio of $n(Ta_2O_5)/n(B_4C)$ decreased from 2.9 to 2.8), contained a trace amount of TaO_2 but no B_4C or C, indicating the expected synthetic reaction of TaB_2 failed to reach completion due to the insufficient amount of reducing agent. On the other hand, upon increasing the ratio of $n(Ta_2O_5)/n(B_4C)$ to 3.0, there existed no oxygen-containing impurity but a minor amount of B_4C remained in the product (MSMBC-5), implying the present addition amount of reducing agent was excessive. So, it was reasonable to conclude that, under the present MSM-BCTR conditions, the optimal molar ratio between Ta_2O_5 and B_4C was approximately 2.9, which was favorable for the completion of the expected synthetic reaction, while minimizing the content of carbon-containing residue in the final TaB_2 product powders.
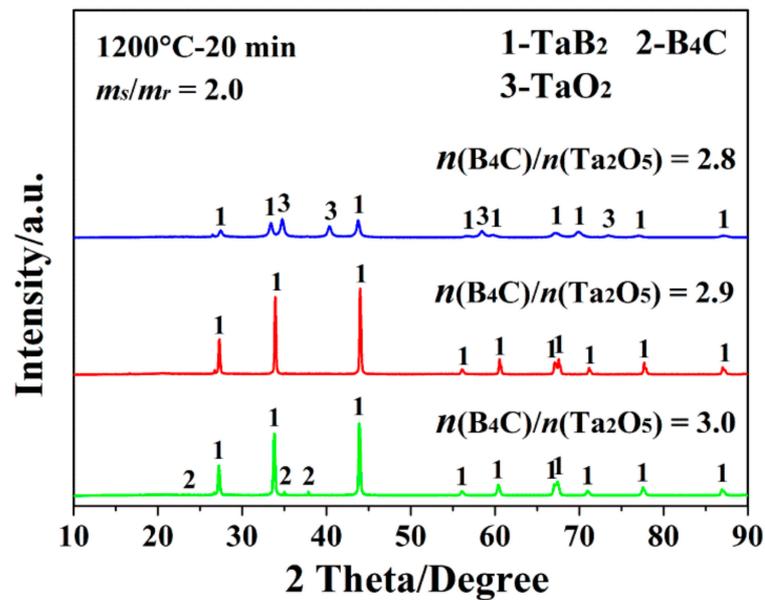
Figure 2. XRD patterns of the samples prepared by MSM-BCTR method at 1200 °C/20 min, with the identical addition amount of salt medium (m_s/m_r = 2.0) and the different molar ratios of B_4C and Ta_2O_5 ($n(B_4C)/n(Ta_2O_5)$) of 2.8–3.0.

Such a prominent achievement of low-temperature and high efficiency preparation of single-phase TaB_2 powders was regarded to be closely related to the specific MSM-BCTR conditions, characterized by microwave heating and salt medium. For the purpose of clarifying their independent impacts on the synthesis of TaB_2, the following experiments were conducted under the optimized processing conditions, without either microwave heating or molten-salt medium, and then compared. On one hand, in the absence of salt medium (corresponding XRD patterns were presented by Figure 3), there existed a small amount of Ta_2O_5 in addition to TaB_2 in the product (MSMBC-6), revealing the molten-salt medium had an obvious positive effect on accelerating the synthetic reaction of TaB_2. On the other hand, in the case of conventional heating (without microwave), multiple types of oxygen-containing impurities (including Ta_2O_5, TaO_2 and TaO), as well as unreacted B_4C, remained in the powder product (MSMBC-7). It was worth noting that TaC, as a common byproduct of TaB_2 synthesized by the conventional BCTR method, was not traced in this sample, although the corresponding synthetic reaction (reaction (2)) remained thermodynamically possible. Such seemingly contradicting results could be explained by the fact that, although reaction (2) prevailed to form TaC, it would be subsequently converted into TaB_2 via reaction (3), which was concurrently enhanced by the molten-salt medium. Therefore, it is reasonable to consider that the combined effects of molten-salt medium and microwave heating had significantly combined effects on the synthesis of TaB_2, including (1) accelerating the targeted reaction by promoting the diffusion coefficients of reacting species and (2) enhancing the thermodynamic favorabilities of the reactions for synthesizing TaB_2 as well as converting intermediate TaC into TaB_2.
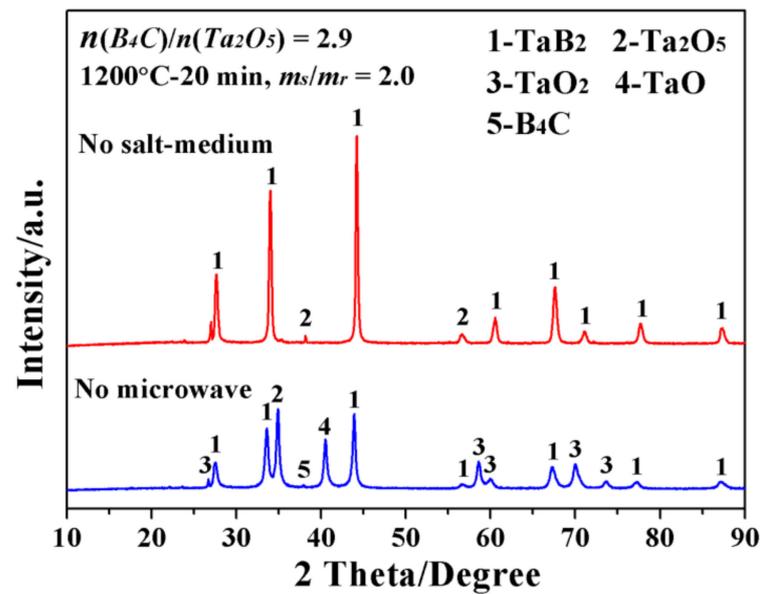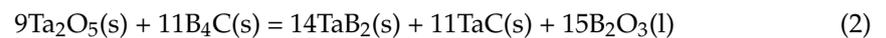
Figure 3. XRD patterns of the samples prepared by MSM-BCTR method under the optimized processing conditions while not using the conditions without using either microwave heating or molten-salt medium.

$$9Ta_2O_5(s) + 11B_4C(s) = 14TaB_2(s) + 11TaC(s) + 15B_2O_3(l) \tag{2}$$

$$7TaC(s) + 2B_4C(s) + 3B_2O_3(l) = 7TaB_2(s) + 9CO(g) \tag{3}$$

Microstructure and morphology of as-prepared phase pure TaB_2 powders (MSMBC-3) were characterized. According to the FE-SEM observation (presented in Figure 4), similar to the TaB_2 synthesized by Shah et al. [23], the particles in this sample exhibited the uniform morphology of urchin-like nanoflowers, which consist of numerous loosely agglomerated nanowires with average diameters and lengths of 410 nm and 4.16 μm, respectively, and a high aspect ratio (>10). Furthermore, the results of EDS-mapping analysis evidence that elements of Ta and B in an atomic ratio close to 2:1, were homogeneously distributed over the as-observed urchin-like nanoflowers, verifying that they were TaB_2 and the as-synthesized TaB_2 powders resulting from the MSM-BCTR were of high purity.
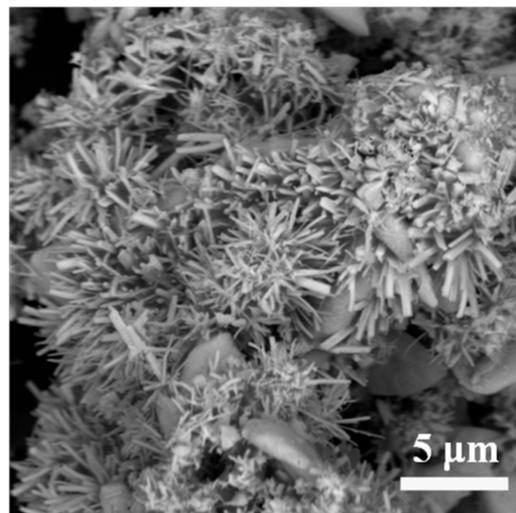

Figure 4. FE-SEM image of the morphology of the TaB_2 powders (MSMBC-3) prepared by MSM-BCTR method at 1200 °C/20 min.

For further revealing the microstructure of as-observed rod-like particles, TEM examination was also conducted. The HRTEM image (Figure 5b, taken in the area defined by a black-dotted circle in Figure 5a) of a well-defined nanowire in an urchin-like nanoflower, shows that a highly arranged atomic lattice and constant interplanar spacings, along the mutually perpendicular directions, of 0.324 nm and 0.265 nm, which matched well with the interplanar spacings of (100) and (001) crystal planes of TaB_2 crystal, respectively. In addition, the SAED pattern (Figure 5c) further verifies that this representative nanowire has a single-crystalline structure, and its anisotropic morphology is formed by epitaxial growth along the [010] direction of the hexagon-system TaB_2 crystal.
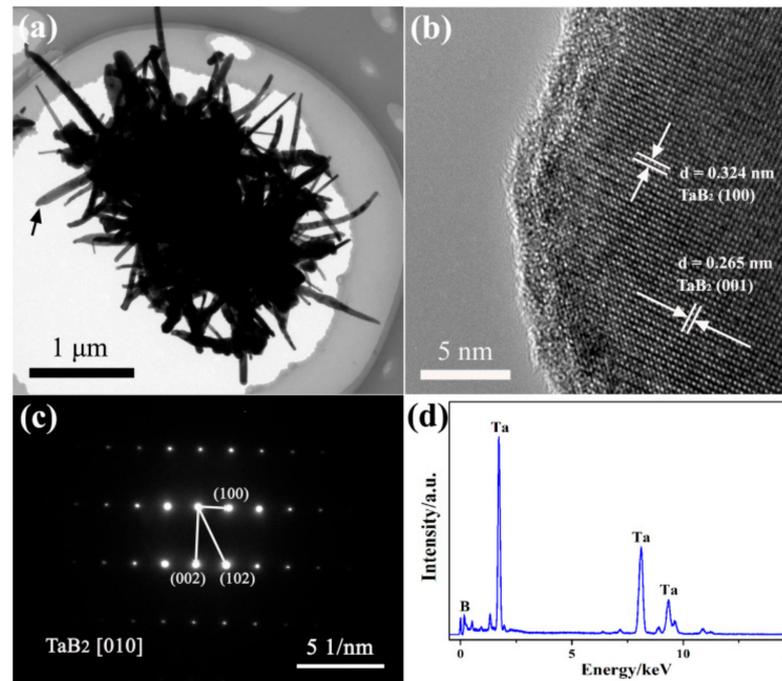

Figure 5. (**a**) Low-resolution TEM image, (**b**) high-resolution TEM image of a representative urchin-like TaB_2 nanoflower in MSMBC-3, (**c**) SAED pattern, and (**d**) EDS of an independent TaB_2 nanowire (marked by a black arrow in (**a**)).

Therefore, it is reasonable to conclude that the TaB_2 powders resulting from the MSM-BCTR method generally had a low extent of aggregation, large specific surface area, single-crystalline nature, and highly oriented anisotropic morphology, which were very favorable for enhancing not only sinterability but also the integral structural performance represented by fracture toughness of their bulk counterparts [24–26]. The achievement of low-temperature, highly efficiency preparation of such high-quality TaB_2 powders can be mainly attributed to the combined effects of molten-salt medium and microwave heating.

Above all, compared to the conventional thermal reduction method, the MSM-BCTR method possessed versatile significant merits in the preparation of TaB_2 and other raw material powder for UHTCs as well as TaB_2, including the low material cost, ultra-high efficiency, low energy consumption, and the potential in optimizing sinterability as well as the overall mechanical properties (especially fracture toughness) of their bulk counterparts, which may shed substantial light on further development of the methodology for industrial production of UHTCs powders.

4. Conclusions

By taking advantage of the highly efficient and energy-saving approach of molten-salt and microwave comodified boro/carbothermal reduction, phase-pure TaB_2 powders were successfully prepared by firing the less expensive raw powders of Ta_2O_5/B_4C at a reduced

temperature of 1200 °C for only 20 min, which were not only remarkably milder than those (firing temperature > 1250 °C and dwell time of dozens of hours) required by the conventional thermal reduction method using the same type of reducing agent, but also much more efficient (at least several hours) even than the methods using a vast amount of strong, but expensive, reducing agent of elemental boron. Moreover, the as-obtained TaB_2 powders exhibited a single-crystalline structure, well-grown morphology of an urchin-like nanoflower, large specific surface area, low agglomeration extent of nanowires with high aspect ratio of >10, and great potential in improving sinterability and toughening their bulk counterparts. Such promising results were mainly attributable to the synergistic effects of molten-salt medium and microwave heating.

Author Contributions: Conceptualization, J.L. and H.Z.; methodology, J.L., P.Y. and D.L.; software, J.L.; validation, J.L., H.Z. and S.Z.; investigation, J.L. and D.L.; resources, J.L.; data curation, J.L. and P.Y.; writing—J.L. and D.L.; writing—review and editing, J.L. and S.Z.; project administration, J.L.; funding acquisition, J.L. and H.Z. All authors have read and agreed to the published version of the manuscript.

Institutional Review Board Statement: Not applicable.

Informed Consent Statement: Not applicable.

Data Availability Statement: For anyone who is interested with the data of this article, please contact with corresponding author.

Conflicts of Interest: The authors declare no conflict of interest.

References

1. Golla, B.R.; Mukhopadhyay, A.; Basu, B.; Thimmappa, S.K. Review on ultra-high temperature boride ceramics. *Prog. Mater. Sci.* **2020**, *111*, 100651. [CrossRef]
2. Fahrenholtz, W.G.; Hilmas, G.E.; Talmy, I.G.; Zaykoski, J.A. Refractory diborides of zirconium and hafnium. *J. Am. Ceram. Soc.* **2007**, *90*, 1347–1364. [CrossRef]
3. Monteverde, F. Resistance to thermal shock and to oxidation of metal diborides-SiC ceramics for aerospace application. *J. Am. Ceram. Soc.* **2007**, *90*, 1330–1338. [CrossRef]
4. Zimmermann, W.J.; Hilmas, G.E.; Fahrenholtz, W.G. Thermal shock resistance of ZrB_2 and ZrB_2-30% SiC. *Mater. Chem. Phys.* **2008**, *112*, 140–145. [CrossRef]
5. Paula, A.; Venugopal, S.; Binner, J.G.P.; Vaidhyanathan, B.; Heaton, A.C.J.; Brown, P.M. UHTC-carbon fibre composites: Preparation, xxyacetylene torch testing and characterisation. *J. Eur. Ceram. Soc.* **2013**, *33*, 423–432. [CrossRef]
6. Zhan, G.D.; Kuntz, J.D.; Wang, J.L.; Mukherjee, A.K. Single-wall carbon nanotubes as attractive toughening agents in alumina-based nanocomposites. *Nature Mater.* **2003**, *2*, 38–42. [CrossRef] [PubMed]
7. Walker, L.S.; Marotto, V.R.; Rafiee, M.A.; Koratkar, N.; Corral, E.L. Toughening in graphene ceramic composites. *ACS Nano* **2011**, *5*, 3182–3190. [CrossRef]
8. Zhang, G.J.; Zou, J.; Ni, D.W.; Liu, H.T.; Kan, Y.M. Boride ceramics: Densification, microstructure tailoring and properties improvement. *J. Inorg. Mater.* **2012**, *27*, 225–233. [CrossRef]
9. Huang, Z.; Liu, J.H.; Huang, L.; Tian, L.; Wang, S.; Zhang, G.; Li, J.Y.; Liang, F.; Zhang, H.J.; Jia, Q.L.; et al. One-step synthesis of dandelion-like lanthanum titanate nanostructures for enhanced photocatalytic performance. *NPG Asia Mater.* **2020**, *12*, 11. [CrossRef]
10. Liu, J.; Liu, J.H.; Zeng, Y.; Zhang, H.J.; Li, Z. Low-temperature high-efficiency preparation of TiB_2 micro-platelets via boro/carbothermal reduction in microwave heated molten salt. *Materials* **2019**, *12*, 2555. [CrossRef]
11. Zhang, S.W. High temperature ceramic materials. *Materials* **2021**, *14*, 2031. [CrossRef] [PubMed]
12. Wang, H.H.; Tian, L.; Huang, Z.; Liang, F.; Guan, K.K.; Jia, Q.L.; Zhang, H.J.; Zhang, S.W. Molten salt synthesis of carbon-doped boron nitride nanosheets with enhanced adsorption performance. *Nanotechnology* **2020**, *31*, 505606. [CrossRef] [PubMed]
13. Guo, W.M.; Zeng, L.Y.; Su, G.K.; Li, H.; Lin, H.T.; Wu, S.H. Synthesis of TaB_2 powders by borothermal reduction. *J. Am. Ceram. Soc.* **2017**, *100*, 2368–2372. [CrossRef]
14. Guo, W.M.; Zhang, G.J. Reaction processes and characterization of ZrB_2 powder prepared by boro/carbothermal reduction of ZrO_2 in vacuum. *J. Am. Ceram. Soc.* **2009**, *92*, 264–267. [CrossRef]
15. Zhang, X.H.; Hilmas, G.E.; Fahrenholtz, W.G. Synthesis, densification, and mechanical properties of TaB_2. *Mater. Lett.* **2008**, *62*, 4251–4253. [CrossRef]

16. Sondhi, A.; Morandi, C.; Reidy, R.F.; Scharf, T.W. Theoretical and experimental investigations on the mechanism of carbothermal reduction of zirconia. *Ceram. Int.* **2013**, *39*, 4489–4497. [CrossRef]

17. Ren, X.R.; Feng, P.Z.; Guo, L.T.; Tao, X.Y.; Li, Z.Y.; Shi, H.L.; Zhang, X.X.; Wang, H. Synthesis of ultra-fine TaB$_2$ nano powders by liquid phase method. *J. Am. Ceram. Soc.* **2017**, *100*, 5358–5362. [CrossRef]

18. Wei, T.T.; Liu, Z.T.; Ren, D.L.; Deng, X.G.; Deng, Q.H.; Huang, Q.; Ran, S.L. Low temperature synthesis of TaB$_2$ nanorods by molten-salt assisted borothermal reduction. *J. Am. Ceram. Soc.* **2018**, *101*, 45–49. [CrossRef]

19. Khan, N.A.; Jhung, S.H. Synthesis of metal-organic frameworks (MOFs) with microwave or ultrasound: Rapid reaction, phase-selectivity, and size reduction. *Chem. Soc. Rev.* **2015**, *285*, 11–23. [CrossRef]

20. Schwenke, A.M.; Hoeppener, S.; Schubert, U.S. Synthesis and modification of carbon nanomaterials utilizing microwave heating. *Adv. Mater.* **2015**, *27*, 4113–4141. [CrossRef]

21. Liu, J.H.; Huang, Z.; Huo, C.G.; Li, F.L.; Zhang, H.J. Low-temperature rapid synthesis of rod-like ZrB$_2$ powders by molten-salt and microwave co-assisted carbothermal reduction. *J. Am. Ceram. Soc.* **2016**, *99*, 2895–2898. [CrossRef]

22. Zeng, Y.; Liu, J.H.; Liang, F.; Xu, H.Y.; Zhang, H.J.; Zhang, S.W. Highly-efficient preparation of anisotropic ZrB$_2$-SiC powders and dense ceramics with outstanding mechanical properties. *J. Am. Ceram. Soc.* **2019**, *102*, 2426–2439.

23. Shah, L.A. Low-temperature molten salt synthesis and characterization of nanowire-like TaB$_2$ powder. *JOM* **2021**, *73*, 1023–1029. [CrossRef]

24. Kuang, X.L.; Liu, T.M.; Zhang, Y.Y.; Wang, W.X.; Yang, M.P.; Zeng, W.; Hussain, S.; Peng, X.H. Urchin-like SnO$_2$ nanoflowers via hydrothermal synthesis and their gas sensing properties. *Mater. Lett.* **2015**, *161*, 153–156. [CrossRef]

25. Emran, M.Y.; Shenashen, M.A.; Eid, A.I.; Selim, M.M.; EI-Safty, S.A. Portable sensitive and selective biosensing assay of dopamine in live cells using dual phosphorus and nitrogen doped carbon urchin-like structure. *Chem. Eng. J.* **2022**, *430*, 132818. [CrossRef]

26. Chen, Y.Z.; Zeng, D.Q.; Zhang, K.; Lu, A.L.; Wang, L.S.; Peng, D.L. Au-ZnO hybrid nanoflowers, nanomultipods and nanopyramids: One-pot reaction synthesis and photocatalytic properties. *Nanoscale* **2014**, *6*, 874–881. [CrossRef] [PubMed]